Molecular insights into the boundary conditions in the Stokes-Einstein relation

Yoshiki Ishii[1] and Norikazu Ohtori[2,*]

[1]*Graduate School of Science and Technology, Niigata University, 8050 Ikarashi 2-no cho, Nishi-ku, Niigata 950-2181, Japan*
[2]*Faculty of Science, Niigata University, 8050 Ikarashi 2-no cho, Nishi-ku, Niigata 950-2181, Japan*

In order to mimic the Brownian particle in liquid, molecular dynamics calculations of dilute solutions of spherical fullerene molecules with various sizes in liquid Ar were performed. To establish the scaling equation for self-diffusion coefficient, D, of the fullerenes, the dependence of D was examined on the mass ratio of solute to solvent and on the energy-parameter ratio used in the Lennard-Jones potentials. The dependence on the energy-parameter ratio remains up to C_{540}, whereas D rapidly becomes independent of the mass ratio with increasing mass of the solute. The product of the scaling equations obtained for the D of the solute and for shear viscosity, η_{sv}, for the solvent gives a relation which replaces the Stokes-Einstein relation based on the hydrodynamics. The present expression does not need both the boundary conditions and the hydrodynamic particle size, but instead the energy-parameter ratio, packing fraction of solvent, and bare size of solute. From the viewpoint of the tackiness at the boundary, the cage correlation function around the diffusing particle was examined; it was found that the decay time of the function depends mainly on the the energy-parameter ratio. Therefore, the energy-parameter ratio accounts for the main part of both the boundary conditions and the hydrodynamic particle size in the Stokes equation, which have so far been ill-defined in any molecular theories.

The Einstein equation for self-diffusion coefficient, D, of Brownian particle in liquid [1] is given as

$$D = \frac{k_B T}{\zeta}, \tag{1}$$

where k_B is the Boltzmann constant, T is the absolute temperature, and ζ is the translational frictional constant on the surface of the particle. The Stokes equation for ζ is given as

$$\zeta = C\eta_{sv} r_S, \tag{2}$$

where C is the constant of 4π or 6π, depending on the boundary conditions, slip or stick, respectively, at the surface of Brownian particle, r_S is the Stokes radius, and η_{sv} is the shear viscosity of liquid surrounding the particle. A combination of these equations is known as the Stokes-Einstein (SE) relation:

$$\frac{D\eta_{sv}}{T} = \frac{k_B}{Cr_S}. \tag{3}$$

Since no interaction between diffusing particles is considered in the SE relation, strictly speaking, it is applicable only to large particles in infinitely dilute solutions. Furthermore, it is assumed that the liquid is a continuum medium in the Stokes equation. In spite of these limitations, however, the SE relation has been regarded as an important benchmark in discussions on transport properties in not only various states of liquids including complex liquids such as colloid [2] and polymer [3] solutions but also aerosols [4]. As a result, the Stokes equation brings two controversies into the discussion: the boundary conditions and the hydrodynamic size of diffusing particle. While the boundary conditions at fluid-solid interfaces have so far been studied extensively in many experimental [5], theoretical [6,7], and simulation [8] works, an ambiguity still

remains between these two parameters when applying the SE relation to these various systems. In other words, these concepts have been ill-defined even in any molecular theories [9]. The related problem can be found also in the dielectric friction in electrolyte solutions [10].

The purpose of the present study is to elucidate a molecular expression which replaces these hydrodynamic expressions. Here we deal with only the translational short-time self-diffusion and will report the results on the rotational diffusion, i.e., the Stokes-Einstein-Debye relation, elsewhere. In addition, systems to be studied are simple ones which comply only with requirements of the original SE relation: dilute solutions of large spherical particles.

In our previous studies [11,12], the relation between D and η_{sv} applicable to simple liquids was derived from molecular dynamics (MD) simulation. The comprehensive expression which holds for a whole range of compositions of binary mixtures of the Lennard-Jones liquids is given as

$$D_i \eta_{sv}/T = (\sigma_i/\sigma_A)^{-1}(\epsilon_i/\epsilon_A)^{-0.2}(m_i/m_A)^{-0.1}$$
$$\times C'(N/V)^{1/3}, \tag{4}$$

where σ and ϵ are the parameters used in the LJ potentials described later, m is the mass of particle, C' is the constant, N is the number of particles included in the system volume V, and subscripts i and A mean the component ($i = 1$ or 2) and the average over both components, respectively. For pure LJ liquids [11], this equation reads simply

$$D\eta_{sv}/T = C'(N/V)^{1/3}, \tag{5}$$

and for infinitely dilute solutions of component 1 [12], it reads

$$D_1 \eta_{sv}/T = (\sigma_1/\sigma_2)^{-1}(\epsilon_1/\epsilon_2)^{-0.2}(m_1/m_2)^{-0.1}$$
$$\times C'(N/V)^{1/3}, \tag{6}$$

*ohtori@chem.sc.niigata-u.ac.jp

where N/V means the number density of the pure liquid of component 2. In these systems, the value of C' is close to $k_B/2\pi$.

The dependence on the terms of σ_1/σ_2, ϵ_1/ϵ_2, and m_1/m_2 derives from that of D. The term $(\sigma_1/\sigma_2)^{-1}(N/V)^{1/3}$ can be rewritten as $\sigma_1^{-1}(6/\pi)^{1/3}\eta^{1/3}$, where η is the packing fraction defined as $(\pi/6)\sigma_2^3 N/V$. Thus, using $C' = k_B/2\pi$, Eq. (6) can be rewritten as

$$\frac{D_1 \eta_{sv}}{T} = \frac{k_B}{2\pi\sigma_1} \times (6/\pi)^{1/3}\eta^{1/3}(\epsilon_1/\epsilon_2)^{-0.2}(m_1/m_2)^{-0.1}. \quad (7)$$

This bare dependence on σ_1^{-1} is common to that in the Eq. (3), which is the core of the SE relation. The additional term of $(6/\pi)^{1/3}\eta^{1/3}$ means the effect of void in liquid which is not considered in the Stokes equation. The term m_1/m_2 means the isotope effect of mass on the self-diffusion coefficient, which has already been accounted for by the perturbation theory [13]. On the other hand, the term ϵ_1/ϵ_2 still remains to be studied.

In the course of molecular approach, we may replace the Brownian particle and the continuum medium assumed in the SE relation with a large spherical molecule and assembly of small molecules, respectively. In order to simulate such a system, we perform MD calculations of various sizes of fullerene in liquid Ar. The distinct differences from the previous study of the LJ liquid mixtures [12] are not only the size of diffusing particles but also the surface condition, which may be sticky or rough, since the fullerenes have many interaction sites on their surfaces with solvent particles. We focus on the dependence of D on the terms of ϵ_1/ϵ_2 and m_1/m_2.

All the MD calculations of fullerenes, C_{20}, C_{60}, C_{180}, C_{240}, or C_{540}, in liquid Ar were performed using the Gromacs 4.5.5 package [14] under NVE conditions, where E was the internal energy. The densities and temperatures simulated along the saturated vapor line of liquid Ar are summarized in Table I. All the bond lengths of C_{60} were fixed at the experimental values [15]. In the other fullerene molecules, the pentagonal bond lengths were set at 0.1450 nm, which is the same as C_{60}. The other hexagonal bond lengths were increased a little so as to keep the spherical topology reported by Tománek [16]. All the C-C distances in the fullerene molecules were constrained with the LINCS algorithm [17]. In all the systems, while the total number of Ar atoms as solvent, N, was 1.6×10^5, that of fullerene molecules was eight. Intermolecular interactions between Ar and fullerenes were evaluated as a

sum of pair potentials between Ar and C atoms within a cutoff distance of 1.2 nm. The interatomic LJ potential was given as

$$\phi_{ArC}(r) = 4\epsilon_{ArC}\left[\left(\frac{\sigma_{ArC}}{r}\right)^{12} - \left(\frac{\sigma_{ArC}}{r}\right)^6\right], \quad (8)$$

where r is the distance between Ar and C atoms and both ϵ_{ArC} and σ_{ArC} were determined using the Lorentz-Berthelot rules [18]: $\sigma_{ArC} = (\sigma_{Ar} + \sigma_C)/2$ and $\epsilon_{ArC} = (\epsilon_{Ar}\epsilon_C)^{1/2}$, where $\sigma_{Ar} = 0.3405$ nm, $\epsilon_{Ar}/k_B = 119.8$ K, $\sigma_C = 0.3469$ nm, and $\epsilon_C/k_B = 33.24$ K. The equations of motion were integrated using the leap-frog algorithm with a time step of 1 fs, and each run consisted of 2×10^6 steps: 2 ns. In each system, after careful equilibration, we performed calculations of 10 runs to obtain D_1 from the different initial configurations, and then evaluated their average and its standard deviation, σ_{SD}. The self-diffusion coefficient of fullerene molecules under a periodic boundary condition, D_1, was calculated using the Einstein relation. Also for the systems containing four fullerene molecules, we have evaluated the self-diffusion coefficient and confirmed that the results agree with those for the systems above stated within the statistical errors. Thus, the effect of collective motion is negligible for the present systems.

The particle size and energy parameter for a fullerene molecule, σ_f and ϵ_f, where $f = C_{20}, C_{60}, C_{180}, C_{240}$, or C_{540}, were estimated, so as to keep a consistency with the previous studies on simple LJ liquids [12], from a potential profile as a function of distance between centers of mass in the Ar atom and fullerene molecule. The distance where the energy was null was defined as $\sigma_{Arf} = (\sigma_{Ar} + \sigma_f)/2$, and the minimum energy of the profile was defined as $\epsilon_{Arf} = (\epsilon_{Ar}\epsilon_f)^{1/2}$. The obtained values for σ_f and ϵ_f are collected in Table II. Hereafter, as σ_1 and ϵ_1 in Eq. (6), these parameters are used in the present discussion. The m_1 in Eq. (6) is simply a sum of the masses of all C atoms included in each fullerene.

The present MD calculations consist of two categories: one includes calculations to determine D_1 of various fullerenes in the same solvent of Ar at the same temperatures and densities, and the other includes calculations to determine each dependence of D_1 on σ_1/σ_2, ϵ_1/ϵ_2, or m_1/m_2 in Eqs. (6) and (7).

Figures 1(a) and 1(b) show the dependence of D_1 on the terms of m_1/m_2 and ϵ_1/ϵ_2 in Eqs. (6) and (7),

TABLE I. Thermodynamic states and related variables of liquid Ar as solvent. T is the temperature (in K), d is the density (in kg m^{-3}), N/V is the number density (in nm^{-3}), L is the side length (in nm) of simulation cell, and η_{sv} and D_{Ar} is the viscosity (in 10^{-4}kgm^{-1}s^{-1}) and diffusion coefficients (in 10^{-9}m^{2}s^{-1}), respectively.

T	d	N/V	η	$(6/\pi)^{-1/3}\eta^{-1/3}$	L	η_{sv}	D_{Ar}
95	1345	20.27	0.419	1.077	19.91	2.00	2.91
107	1263	19.03	0.393	1.100	20.33	1.48	4.43
120	1160	17.49	0.362	1.131	20.92	1.06	6.66
130	1065	16.05	0.332	1.164	21.52	0.85	9.05
140	942	14.20	0.293	1.213	22.42	0.63	12.60

TABLE II. The size and energy parameters for rare gas atoms and fullerenes as solutes.

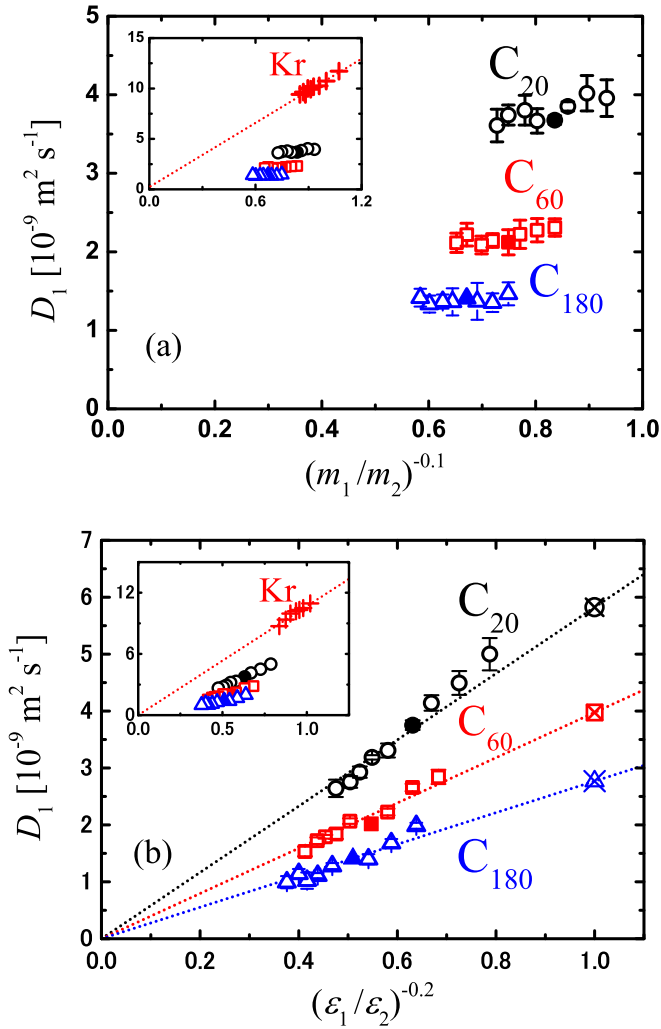| Solute	σ_1 [nm]	$\epsilon_1 k_B^{-1}$ [K]	(σ_1/σ_2)	$(\epsilon_1/\epsilon_2)^{0.2}$	$(m_1/m_2)^{0.1}$
Rare gas atoms					
Ar	0.3405	119.8	1.000	1.000	1.000
Kr	0.3670	167.0	1.078	1.069	1.077
Xe	0.3924	257.4	1.152	1.165	1.126
Fullerenes					
C_{20}	0.614	1197	1.802	1.585	–
C_{60}	0.914	2448	2.683	1.828	–
C_{180}	1.478	3476	4.339	1.961	–
C_{240}	1.694	3746	4.974	1.991	–
C_{540}	2.412	4155	7.082	2.032	–

FIG. 1. Dependence of the self-diffusion coefficient of some sizes of fullerenes and Kr in liquid Ar on (a) the mass ratio and (b) the energy-parameter ratio of solute to solvent. In (b), the plots at $\epsilon_1/\epsilon_2 = 1$ mean simply those for the extrapolated values of D_1.

FIG. 2. Plots of $D_1 \eta_{sv}/T$ vs (a) σ_1^{-1} and (b) $(\sigma_1/\sigma_2)^{-1}$ $(\epsilon_1/\epsilon_2)^{-0.2}(N/V)^{1/3}$. The multiple plots for the same symbol mean the different temperatures shown in Table I.

respectively. These results clearly show that, while the mass-ratio dependence vanishes with increasing mass of fullerene, the same dependence as Eqs. (6) and (7) on the ratio of the energy parameters remains up to C_{180}. In our previous study [12], we showed that the dependence on the mass ratio has the same origin with the isotope effect of mass on the self-diffusion coefficient. The effect can be explained by the perturbation theory on the small difference between masses [13]. In addition, since the theory tells also that the effect vanishes with increasing mass difference, the observed behavior is a natural consequence. Therefore, we conclude that the mass-ratio term can be negligible in fullerenes, and hereafter we exclude the mass-ratio term from the discussion about fullerenes. In Fig. 1(b) the virtual values of D_1 at $\epsilon_1/\epsilon_2 = 1$ were estimated for each fullerene by extrapolation of the dependence, which will be discussed later.

Figures 2(a) and 2(b) compare two expressions for $D_1 \eta_{sv}/T$. Figure 2(a) based on the original SE relation shows that, whereas Ar in liquid Ar seems to behave under the slip
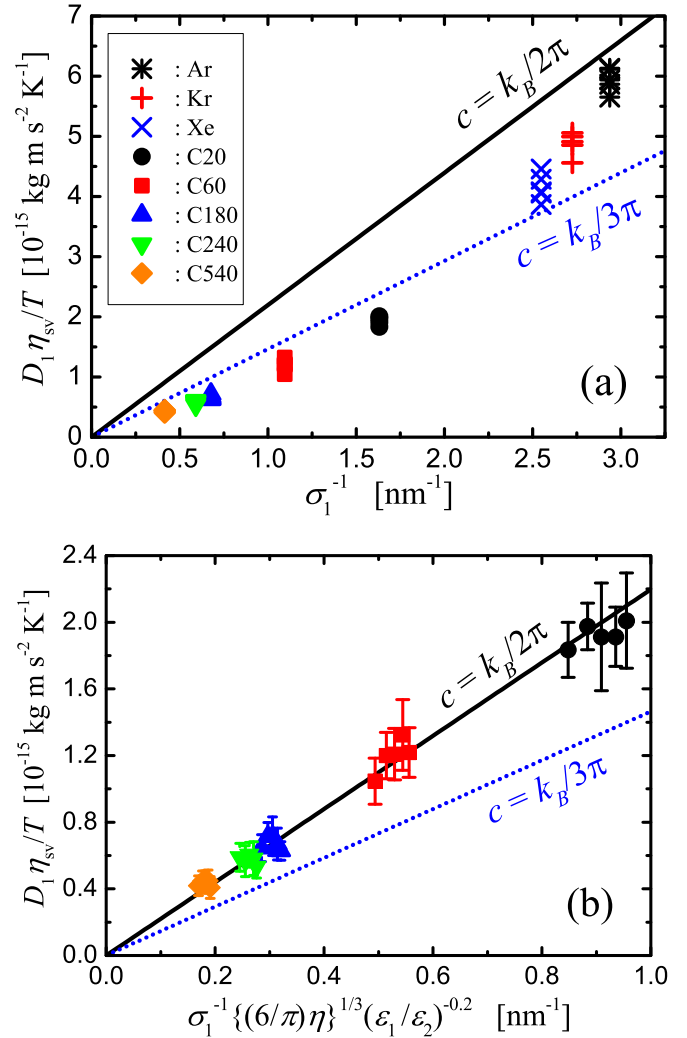
boundary condition, the fullerenes do under the stick boundary condition. These seem to agree with expectations from the Stokes law. However, the plots for Kr and Xe in liquid Ar seem to deviate significantly from the slip boundary condition. Furthermore, in fact, even those for the fullerenes significantly deviate from the stick boundary condition as discussed later. On the other hand, Fig. 2(b) shows that these results follows consistently

$$\frac{D_1 \eta_{sv}}{T} = \frac{k_B}{2\pi \sigma_1} \times (6/\pi)^{1/3} \eta^{1/3} (\epsilon_1/\epsilon_2)^{-0.2}. \qquad (9)$$

In addition, as shown in the previous study [12], D_1 of rare gas atoms follows Eqs. (6) and (7). Thus, all the D_1 follows Eq. (7) or (9) with the same slope, i.e., without any modifications by the boundary conditions. The plot of $D_1 \eta_{sv}/T$ versus $(\sigma_1)^{-1}(6/\pi)^{1/3} \eta^{1/3}$, using D_1 extrapolated at $\epsilon_1/\epsilon_2 = 1$ shown in Fig. 1(b), also clearly follows the line with the same slope, as shown in Fig. 3. This definitely shows that, conversely, deviations of ϵ_1/ϵ_2 from unity cause the deviations from the line with slope of $k_B/2\pi$ in the original SE relation.
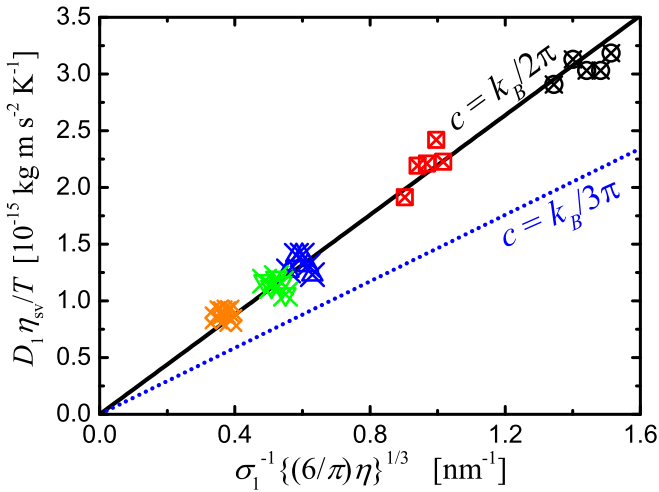
FIG. 3. Plots of $D_1\eta_{sv}/T$ using D_1 extrapolated at $\epsilon_1/\epsilon_2 = 1$ vs $(\sigma_1/\sigma_2)^{-1}(N/V)^{1/3}$. The multiple plots for the same symbol mean the different temperatures shown in Table I.

FIG. 5. Dependence of the decay time of half of the cage surrounding the fullerene molecules or rare gas atoms in liquid Ar on $(\epsilon_1/\epsilon_2)^{-0.2}$. The decay time was evaluated for the same values of $(\epsilon_1/\epsilon_2)^{-0.2}$, which is used in Fig. 1(b). The inset shows the decay time simply for all the kinds of solutes.

Next, we discuss another option in the molecular interpretation of the SE relation: hydrodynamic particle size. Applying Eq. (3) to the present results, we can obtain the apparent or hydrodynamic molecular size, which depends on the boundary conditions. Figure 4 compares the apparent diameter derived from Eqs. (3) and (9). While Eq. (9) gives always very close values to σ_1, Eq. (3) gives about 30% larger values than σ_1 for large fullerenes even under the stick boundary condition. The increase in the apparent size under the slip boundary condition can be explained by a product between the packing fraction and the energy-parameter terms, which are numerically shown in Tables I and II, respectively.

All the problems discussed above arise from Eq. (2) and vanish simply if Eq. (2) is replaced with

$$\zeta = 2\pi\eta_{sv}\sigma_1(6/\pi)^{-1/3}\eta^{-1/3}(\epsilon_1/\epsilon_2)^{0.2}. \quad (10)$$
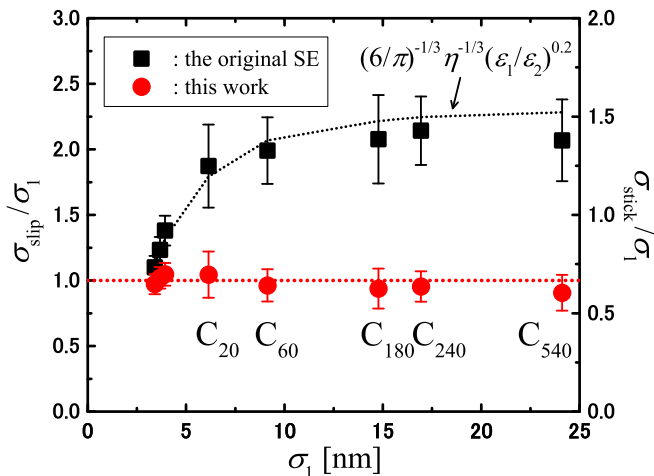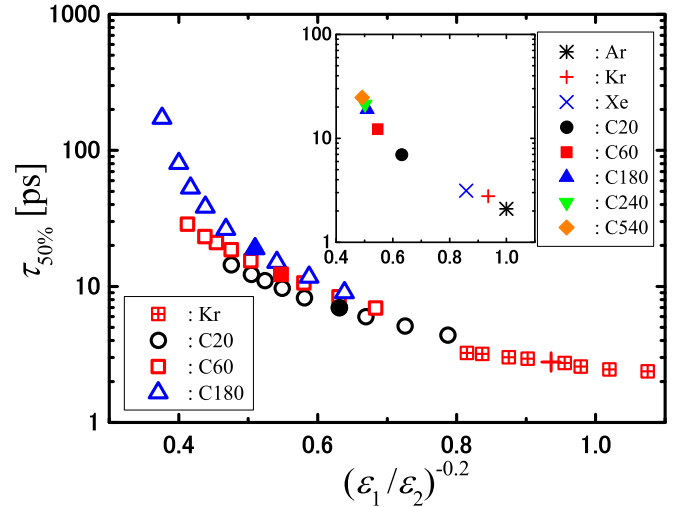

FIG. 4. Hydrodynamic size of the solute molecules in liquid Ar at 120 K. The left and right axes correspond to the slip and stick boundary conditions, respectively.

This is the unambiguous molecular expression for the friction constant of large spherical particles in a simple liquid. This equation holds for both rough and smooth surfaces [19]. Since correct evaluations of the friction constant using numerical simulations have so far been supposed to be not easy [20], the present approach can be another option for studies of the friction constant at any interfaces.

Last, in order to clarify the effect of the ϵ_1/ϵ_2 term on the boundary between solute and solvent, we evaluated the normalized cage correlation function with respect to the diffusing particles, where the radius of cage was defined as the first minimum of pair distribution function between fullerene and Ar. Figure 5 shows the dependence on the ϵ_1/ϵ_2 term of the decay time of 50% of cage surrounding the diffusing particles. Note that, while the open symbols show the dependence on the artificial variation of $(\epsilon_1/\epsilon_2)^{-0.2}$, the closed symbols show the decay times for the original values of $(\epsilon_1/\epsilon_2)^{-0.2}$ shown in Table II, as inverse. The figure shows clearly that the decay time decreases, i.e., its sticky property increases, with increasing $(\epsilon_1/\epsilon_2)^{-0.2}$. A more important point is that, in spite of the difference in materials, i.e., size or mass, the same value of ϵ_1/ϵ_2 produces almost the same level of decay time. This means that the decay time is a function mainly of the energy-parameter ratio. As shown in Tables I and II, the weight of the ϵ_1/ϵ_2 term is much larger than that of packing-fraction term. Therefore, we can conclude that the ϵ_1/ϵ_2 term in Eq. (10) accounts for the main part of both the boundary conditions and the hydrodynamic particle size in Eq. (2).

[1] A. Einstein, *Investigation on the Theory of the Brownian Movement* (Dover, New York, 1956).

[2] R. M. Mazo, *Brownian Motion: Fluctuations, Dynamics, and Applications* (Oxford University Press, New York, 2002).

[3] T.-H. Fan, J. K. G. Dhont, and R. Tuinier, Phys. Rev. E **75**, 011803 (2007).

[4] Z. Li and H. Wang, Phys. Rev. E **68**, 061206 (2003).

[5] C. Neto, D. R. Evans, E. Bonaccurso, H.-J. Butt, and V. S. J. Craig, Rep. Prog. Phys. **68**, 2859 (2005).

[6] T. Keyes and A. J. Masters, Adv. Chem. Phys. **58**, 1 (1985).

[7] J. L. Barrat and L. Bocquet, Phys. Rev. Lett. **82**, 4671 (1999).

[8] P. A. Thompson and S. M. Troian, Nature (London) **389**, 360 (1997).

[9] J. T. Hynes, R. Kapral, and M. Weinberg, J. Chem. Phys. **70**, 1456 (1979).

[10] P. G. Wolynes, J. Chem. Phys. **68**, 473 (1978).

[11] N. Ohtori and Y. Ishii, Phys. Rev. E **91**, 012111 (2015).

[12] N. Ohtori and Y. Ishii, J. Chem. Phys. **143**, 164514 (2015).

[13] I. Binas and I. Mryglod, Condens. Matter Phys. **12**, 647 (2009).

[14] B. Hess, C. Kutzner, D. van der Spoel, and E. Lindahl, J. Chem. Theory Comput. **4**, 435 (2008).

[15] C. S. Yannoni, P. P. Bernier, D. S. Bethune, G. Meijer, and J. R. Salem, J. Am. Chem. Soc. **113**, 3190 (1991).

[16] D. Tománek, *Guide through the Nanocarbon Jungle* (Morgan & Claypool, San Rafael, 2014).

[17] B. Hess, H. Bekker, H. J. C. Berendsen, and J. G. E. M. Fraaije, J. Comput. Chem. **18**, 1463 (1997).

[18] M. P. Allen and D. J. Tildesley, *Computer Simulation of Liquids* (Oxford Science, New York, 1989).

[19] D. Chandler, J. Chem. Phys. **60**, 3500 (1974).

[20] S. H. Lee and R. Kapral, J. Chem. Phys. **121**, 11163 (2004).